Mechanisms of surface antigenic variation in the human pathogenic fungus *Pneumocystis jirovecii*

Emanuel Schmid-Siegert [1], Sophie Richard [2], Amanda Luraschi [2], Konrad Mühlethaler [3], Marco Pagni [1], Philippe M. Hauser [2]

[1] Vital-IT Group, SIB Swiss Institute of Bioinformatics, Lausanne, Switzerland

[2] Institute of Microbiology, Lausanne University Hospital, Lausanne, Switzerland

[3] Institut für Infektionskrankheiten, Universität Bern, Bern, Switzerland

Corresponding author :
P. Hauser
Av. Bugnon 48
IMUL CHUV
1011 Lausanne
Phone +41 21 314 40 84
Philippe.Hauser@chuv.ch

Running title : Antigenic variation in *Pneumocystis jirovecii*

Words text: 5180

Methods text: 2028

Abstract: 268

Keywords: *Pneumocystis carinii*, PCP, major surface glycoprotein, adhesin, subtelomere, mosaicism, PacBio sequencing.

Abstract

Background: Microbial pathogens commonly escape the human immune system by varying surface proteins. Here we investigated the mechanisms used for that purpose by *Pneumocystis jirovecii*. This uncultivable fungus is an obligate pulmonary pathogen which causes pneumonia in immuno-compromised individuals, a major life-threatening infection.

Results: Long-read PacBio sequencing was used to assemble a set of subtelomeres of a single *P. jirovecii* strain from a bronchoalveolar lavage fluid specimen of a single patient. A total of 113 genes encoding surface proteins were identified, including 28 pseudogenes. These genes formed a subtelomeric gene superfamily which included five families encoding adhesive GPI-anchored glycoproteins, and one family encoding excreted glycoproteins. Numerical analyses suggested that diversification of the glycoproteins relies on mosaic genes created by ectopic recombination, and occurs only within each family. DNA motifs suggested that all genes are expressed independently, except those of the family encoding the most abundant surface glycoproteins which are subject to mutually exclusive expression. PCR analyses showed that exchange of the expressed gene of the latter family occurs frequently, possibly favoured by the location of the genes proximal to the telomere because this allows concomitant telomere exchange.

Conclusions: Our observations suggest that (i) the structure of *P. jirovecii* cell surface is made of a complex mixture of different glycoproteins, (ii) genetic mosaicism ensures variation of the glycoproteins, and (iii) the strategy of the fungus consists in the continuous production of new subpopulations composed of cells which are antigenically different. This strategy is unique among human pathogens and may be associated to the particular niche within lungs which tolerates the presence of low abundant fungi within the natural microbiota.

Introduction

Pneumocystis jirovecii is a fungus colonizing specifically human lungs. It has developed strategies to survive in healthy human lungs, at least transiently, and can turn into a deadly pathogen causing pneumonia in individuals with debilitated immune system (Cushion et al. 2007; Cushion and Stringer 2010; Hauser 2014; Ma et al. 2016). This disease is the second most frequent life-threatening invasive fungal infection with ca. 400'000 cases per year worldwide (Brown et al. 2012). However, the biology of this pest remains difficult to study in the lab because of the lack of any established methods for *in vitro* culture. Recent progresses in understanding *P. jirovecii* biology strongly benefitted from the publication of two assemblies of its genome from two different clinical samples (Ma et al. 2016; Cissé et al. 2012).

In contrast to other pathogenic fungi, the cells of *P. jirovecii* lack chitin as well as glucans during part of the cell cycle, which may avoid eliciting innate and acquired immune responses (Ma et al. 2016). Moreover, a mechanism of surface antigenic variation, to which ca 5% of the genome is dedicated (Ma et al. 2016), seems crucial to escape from the human immune system during colonisation, although it has not been understood in details so far. Surface antigenic variation is a common strategy among major microbial human pathogens, for example in *Plasmodium*, *Trypanosoma*, *Candida*, *Neisseria*, and *Borrelia*. It relies on various genetic and/or epigenetic mechanisms aimed at expressing only one or few of them at once (Deitsch et al. 2009). Such systems often involve gene families encoding surface antigens localized at subtelomeres, presumably because these regions of the genome are prone to gene silencing, which is used for mutually exclusive expression, and possibly to enhanced mutagenesis (Barry et al. 2003). Moreover, the formation of clusters of telomeres at the nuclear periphery may favour ectopic recombinations (Barry et al. 2003), which can be responsible for the generation of new mosaic antigens.

Surface antigenic variation has been previously studied on a limited set of genes in *Pneumocystis carinii* infecting specifically rats. The molecular mechanism was then assumed to be also active in *P. jirovecii*, as suggested by studies using PCR-based technologies. Antigen diversity was believed to be generated by recombination between members of a single family of ca. 80 subtelomeric genes encoding isoforms of the major surface glycoprotein (*msg*) (Keely et al. 2005; Keely et al. 2009; Stringer 2007). A single of these isoforms would be expressed in each cell thanks to its localization downstream of a subtelomeric expression site, the upstream conserved element (UCS) present at a single copy in the genome. The UCS includes the promoter of transcription, the protein start, and the leader sequence responsible for translocation of the protein into the endoplasmic reticulum for final incorporation into the cell wall (Kutty et al. 2001; Kutty et al. 2013). The mechanism for exchange of the expressed *msg* gene is thought to be by recombination at a 33 bps long sequence which is present both at the end of UCS and beginning of each *msg* (the conserved recombination junction element, CRJE). The exchange of the expressed gene seems relatively frequent and would explain how different *msg* genes can be expressed in each population (Kutty et al. 2001). The CRJE sequence encodes at its end a potential lysine-arginine recognition site for Kexin endonuclease which might be involved in the maturation of the antigen. Kutty *et al* (Kutty et al. 2008) provided evidence for frequent recombinations among *msg* genes creating potentially mosaic genes. All these observations were made using conventional cloning procedures and PCRs, and these mechanisms have yet to be understood in a more extensive genomic context.

The first genome sequence of *P. jirovecii* released was obtained using technologies generating short reads which prevented assembly of long repetitive sequences such as centromeres, telomeres, and subtelomeres including *msg* genes (Cissé et al. 2012). A second study used a mixture of techniques which generated more complete chromosomes of *P. jirovecii*, *P. carinii*,

and *Pneumocystis murina* (infecting specifically mice) (Ma et al. 2016). These latter authors used PCRs coupled with long read sequencing to reconstruct the subtelomeres. This allowed discovering new subtelomeric gene families related to *msg*. The number of these families as well as the number of their members present in each *Pneumocystis* species varied. They further described the specific arrangement of the members of each family within the subtelomeres, and suggested, based on RNA sequencing, that all *msg* genes are expressed in a given population of *P. carinii* or *P. murina*. However, they did not discuss the function of these proteins, the mechanisms involved in their expression and gene variation, or the global strategy of antigenic variation of these fungi.

The aim of the present study was to analyse in details the mechanisms of surface antigenic variation in *P. jirovecii*. To that purpose, we used the PacBio sequencing technology generating long DNA reads to assemble a set of subtelomeres of a single *P. jirovecii* strain from a bronchoalveolar lavage fluid specimen (BALF) of a single patient. The analysis of this dataset and laboratory experiments permit a new classification and the characterization of six subtelomeric *msg* families, demonstrate the presence of pseudogenes, and provide important new insights into the molecular mechanisms responsible for antigenic variation. Moreover, our observations suggest a unique strategy of antigenic variation consisting in the continuous production of new subpopulations composed of cells which are antigenically different. This strategy may be associated to the particular non-sterile niche within lungs.

Results

Most if not all *P. jirovecii* infections are polyclonal (Alanio et al. 2016). In order to facilitate the study of the mechanisms of antigenic variation, one patient infected with a vastly dominant strain was selected by multitarget genotyping. The genome of a single *P. jirovecii* strain was assembled into 219 contigs using PacBio sequencing and a dedicated bioinformatics strategy for reads processing.

Identification of subtelomeric *msg* genes and pseudogenes

Automated gene prediction performed poorly in the subtelomeric regions as compared to the core of the genome, due to abundant stretches of low-complexity DNA, numerous pseudogenes, residual assembly errors in homopolymers, and the lack of a start codon in many *msg* genes. The *msg* genes were detected by sequence homology using generalized profiles (Bucher and Bairoch 1994) derived from previously published sequences. A total of 113 *msg* genes with sizes ranging from 331 to 3337 bps were found on 37 different contigs, only two genes being perfectly identical (*msg* 52 and 61, Additional file 1: Table S1). Most of them (N=85) contained a single large exon and zero to two small exons at their 5' end. The remaining 28 genes harboured many stop codons in all frames and were considered as pseudogenes (Additional file 2: supplementary note 1).

Characterization of the *msg* gene families

We are proposing a classification of the *msg* genes into six families (Table 1) based on of the integration of four independent lines of evidence: sequence homology, gene structure, protein property, and recombination events. The global picture that emerged is coherent and the details on the different points are presented below.

Table 1. Characteristics of the *msg* families identified in *P. jirovecii*.

		Gene							Protein							
										C-terminus						
Family name	Color in figures	No. genes full-length / partial / pseudo-	Mean full-length (bps) ± st dev	Location in subtelomere relatively to telomere	Presumptive TATA box (bps to ATG, range)	CRJE	No. 5'-end introns	Average pairwise identity (%) ± st dev	Signal peptide	ST-rich region	ST-rich region	PE-rich region	GPI-anchor signal	No. N-glycosylation site	Average pairwise identity (%) ± st dev	Corresponding Ma et al (2016) family [a]
msg-I		11 / 16 / 16	3071 ± 39	proximal	- [b]	+	0	71 ± 7	- [b]	+	+	-	+	4-10	54 ± 8	*msg*-A1
msg-II		11 / 3 / 4	3155 ± 31 [c]	central	21-28	-	2	83 ± 13	+	+	+	-	+	2-14	73 ± 16	*msg*-A3
msg-III		7 / 2 / 1	3146 ± 55	central	18-24	-	2	83 ± 10	+	+	+	-	+	7-11	70 ± 13	*msg*-A3
msg-IV		6 / 1 / 2	2023 ± 45	central	29-36	-	1	72 ± 14	+	-	-	-	-	0-8	49 ± 17	*msg*-B
msg-V		8 / 6 / 1	3056 ± 126	central	30-67	-	1	66 ± 5	+	-	+	+	+	5-12	44 ± 4	*msg*-D
msg-VI		6 / 1 / 0	1222 ± 189	distal	33-56	-	1	45 ± 7	+	-	+	+	+	0-1	21 ± 5	*msg*-E
msg outlier		6 / 1 / 4	variable	central/distal	NA [d]	+/-	variable	NA	+/-	+/-	+/-	-	+/-	variable	NA	NA

[a] The family *msg*-C described by Ma et al (2016) was not identified here (Supplementary note 6).

[b] The promoter including the signal peptide for this family is within the UCS present at a single copy per genome.

[c] The *msg*3 gene was not used to calculate this value because it is ca. 900 pbs shorter than the other genes of the family, although it presents all features of the family (see alignment in Figure S2).

[d] Not applicable.

Figure 1a shows the results of the analysis of 61 *msg* genes containing an exon equal or larger than 1.6 kb. Based on the multiple sequence alignments (MSAs) of the CDS and of their predicted proteins, two phylogenetic trees were computed using RAxML. The different gene families are clearly individualised as clades, with the exceptions of (i) *msg*-II which appears as a sub-clade of *msg*-I, and (ii) *msg*-I which seems to include two sub-clades. Using an alternative classification method that does not rely on a single particular MSA (JACOP, Fig. 1a), the placement of *msg*-II as a sub-clade of *msg*-I was not confirmed, whereas the sub-clades of *msg*-I were. Owing on the differences in the gene structures and on the recombination events reported below, we believe that (i) *msg*-I and *msg*–II should be treated separately, and (ii) *msg*-I should be considered as a single family including two sub-clades. Figure 1b shows the analysis of trimmed CDS sequences allowing the placement of the *msg*-VI family which appeared as a clade on its own, while the classification of the other families remained essentially unchanged. Figure S1 shows that most pseudogenes could be attributed to one *msg* family and their often longer branches further account for their pseudogenic nature (Additional file 2).

Manual curation of the *msg* genes led to their classification in full-length, partial, and pseudogenes (Table S1). Table 1 shows the characteristics of each family identified by the analysis of the sequences of the full-length genes, as well as of their alignments (Fig. S2). Except those of the family *msg*-I, each *msg* gene presented one or two introns at its 5’ end, as well as a presumptive TATA box upstream of the ATG and an initiator motif (Cap signal) at presumptive sites of initiation transcription (Fig. 2a and S2). The members of the family I had only the conserved recombination junction element (CRJE) at the beginning of their single exon. These observations suggested that members of family I can be expressed only upon recombination of

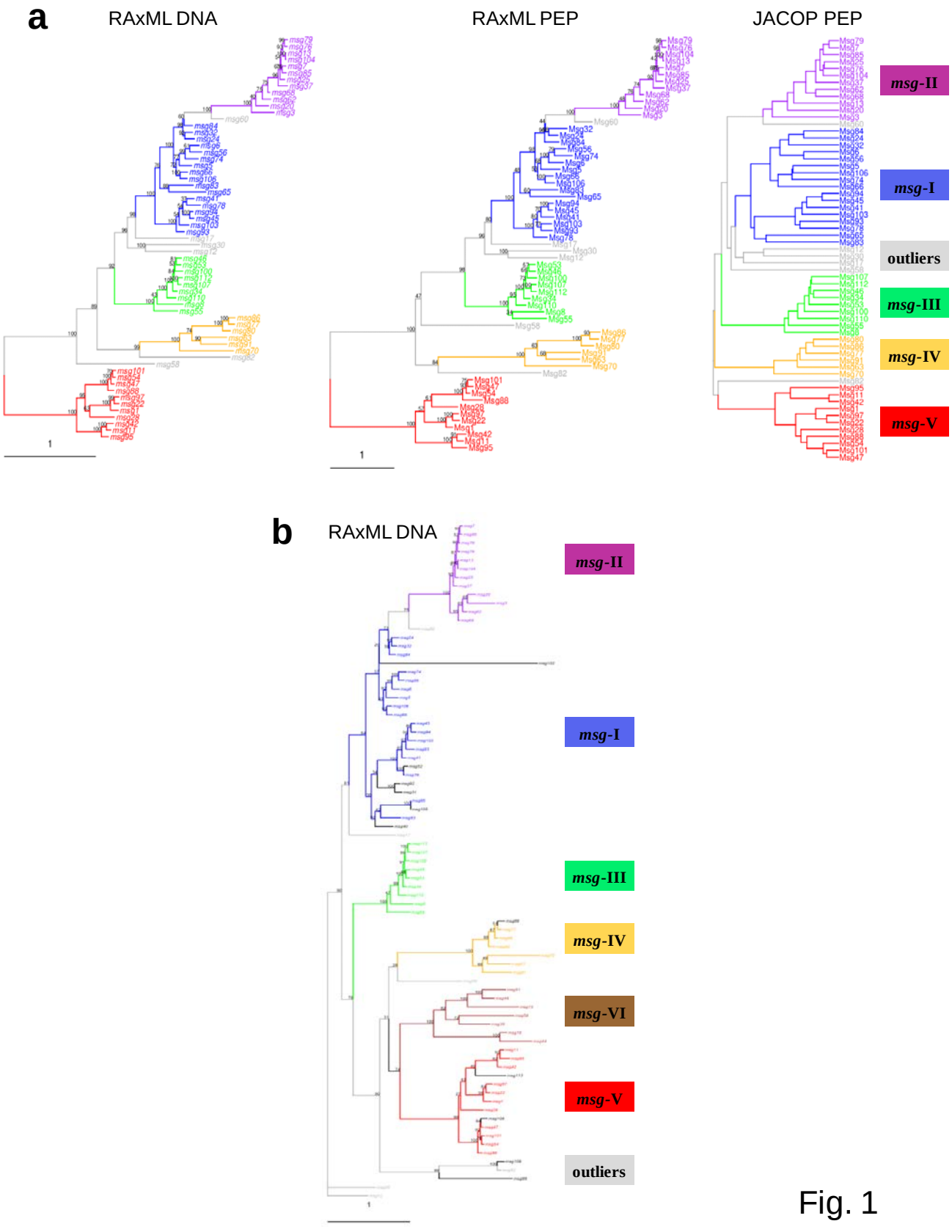

Fig. 1

Fig. 1

Classification trees of *P. jirovecii msg* genes and Msg proteins. The different families are represented in colours and their characteristics are summarised in Table 1. A few unclassified outliers are in grey. Scale, mean substitution / site. (**a**) RAxML DNA and PEP are maximum likelihood trees of nucleotide and amino acid sequences of the 61 genes with an exon larger than 1.6 kb. Members of family V were defined as the out-group (1000 bootstraps). JACOP PEP is a hierarchical classification based on local sequence similarity, a method that does not rely on a particular multiple sequence alignment. (**b**) Maximum likelihood tree of the 61 genes with an exon larger than 1.6 kb, plus 18 genes with an exon smaller than 1.6 kb. The sequences were trimmed from position 1540 of the first alignment up to their end, and re-aligned to construct the tree (1000 bootstraps). Seven of the 18 genes with an exon smaller than 1.6 kb constitute the *msg* family VI shown in brown, whereas the remaining 11 shown in black belong to the other *msg* families.

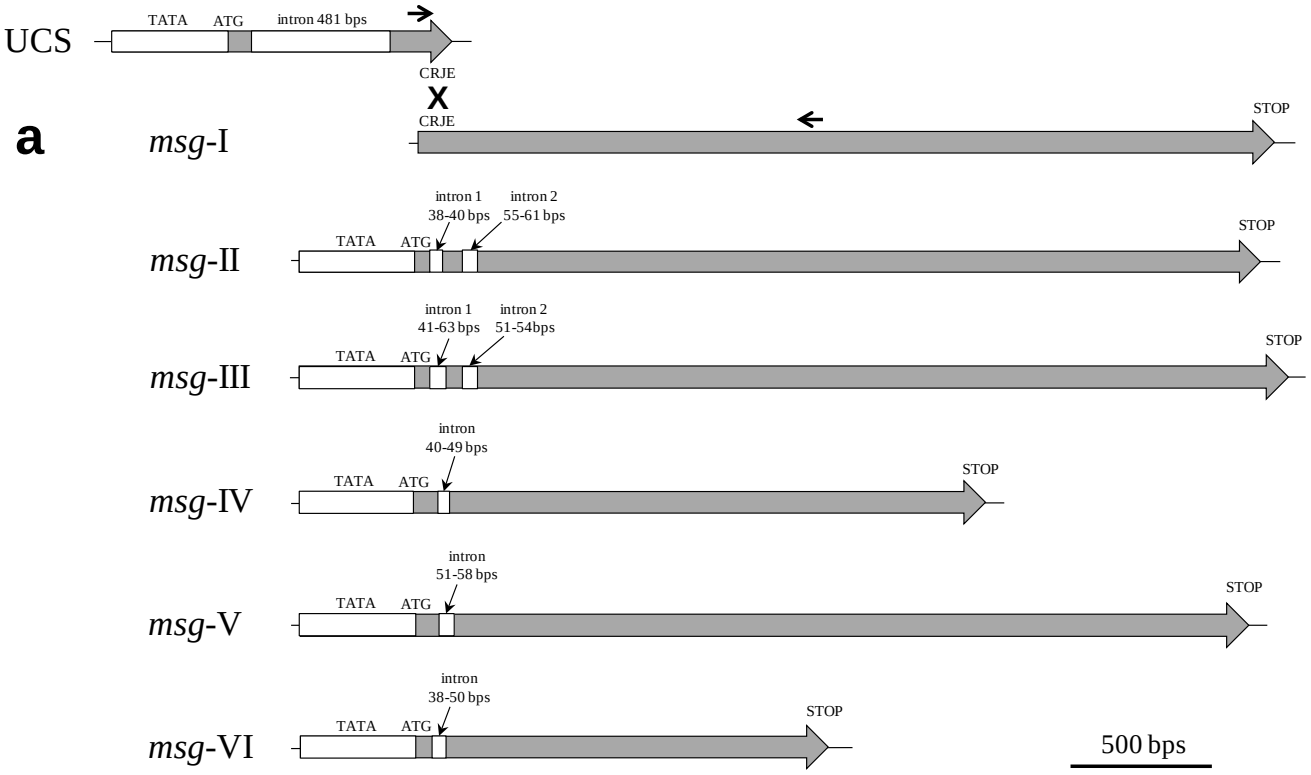

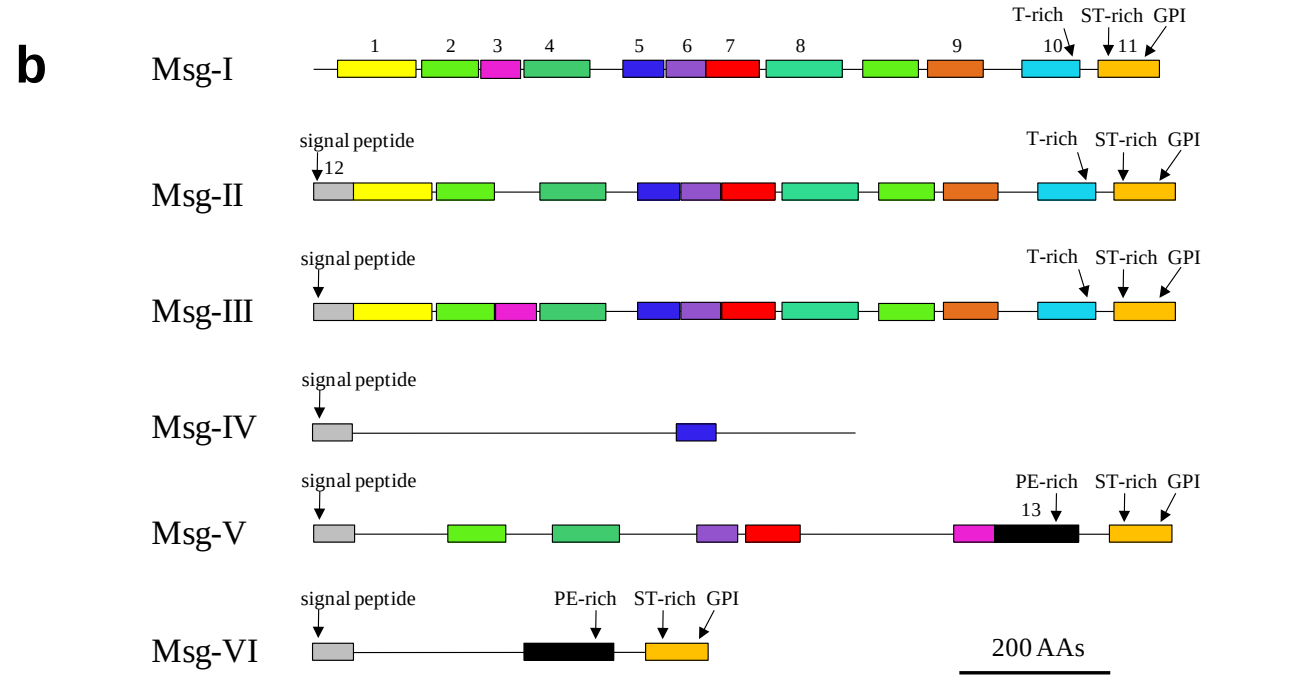

Fig. 2

Fig. 2

Diagrams of the structure of *P. jirovecii msg* genes and Msg proteins belonging to six families. (**a**) Features of the *msg* genes of each family derived from the analysis of the full-length genes. The UCS and recombination between CRJE sequences are figured. The approximate position of PCR primers used for identification of the *msg*-I expressed genes linked to the UCS are shown by arrows (Supplementary note 4). (**b**) Features of Msg proteins of each family derived from the analyses of the full-length proteins. The 13 domains identified using MEME analysis are shown. The logos of these domains are shown in Figure S4.

their CRJE with that of the single copy UCS which encompasses a promoter, whereas all members of the other five families are expressed independently. Three of the six full-length outlier genes seemed not expressed since they had no CRJE and missed a TATA box (Table S1). Twenty-six partial genes were truncated by the end of the contig so that only three *bona fide* partial genes were identified, which, however, missed TATA box, signal peptide, and/or GPI-anchor signal, and thus were probably not expressed or not correctly processed (*msg* 44, 89, and 99).

Characterization of the Msg protein families

Analysis of the sequences and alignments (Fig. S3) of the full-length proteins of each family revealed that each Msg protein, except those of family I, presented a signal peptide at its N-terminus (Fig. 2b). Proteins of family I probably acquire a signal peptide upon fusion of their encoding gene with the UCS. Except those of family IV, each Msg protein presented a GPI-anchor signal at its C-terminus. These observations suggested that all Msg proteins are attached externally to the cell wall, except those of family IV which would be secreted in the environment or attached to the cell wall through another mechanism than GPI.

The possible conservation of motifs among the proteins of the six families was investigated using Multiple Expectation–Maximization for Motif Elicitation (MEME analysis) (Bailey and Elkan 1994). Thirteen conserved motifs were identified which arrangement was fairly diagnostic within each family (Fig. 2b). Most motifs included several conserved cysteines and leucines, which resembled to the previously identified Pfam MSG domain (Fig. S4). Interestingly, conserved leucines were often separated by two to six residues. The beginning of motif 10 corresponded to the end of the previously identified Pfam Msg2_C domain. Accordingly, Pfam

predictions identified one to five MSG domains, often partial, per protein of all families, and a single Msg2_C domain in each Msg-I protein (Fig. S5; Table S2). The Msg2_C domain was not predicted in families II and III although they harboured the corresponding motif 10, suggesting that this domain is divergent in these families. Ncoils predictor revealed three to five coiled-coil motifs spread along members of families I, II, and III, whereas unstructured regions were predicted at the C-terminus of Msg proteins of families I, III, V, and VI (Fig. S5).

Except those of family IV, each Msg protein harboured at its C-terminus two MEME motifs which included a region enriched in specific residues: threonine (T-rich; motif 10), serine and threonine (ST-rich; 11), or proline and glutamine (PE-rich; 13)(Fig. 2b; Table 1). The T-rich region in family I included generally a stretch of nine to 15 Ts, which was not present in families II and III (Fig. S3). The PE-rich region in family V was enriched in proline residues relatively to that present in family VI (Fig. S3). Four to 14 potential sites of nitrogen-linked glycosylation of asparagines were predicted to be present in each Msg protein, except in family VI which presented no or only one such site (Table 1; Fig. S3). The localization of these glycosylation sites was widespread along the protein and fairly conserved within each family.

Arrangement of the *msg* families within the subtelomeres

Consistent with subtelomeric localization, the *msg* genes were grouped at one end of their contig when flanking non-*msg* genes were also present (in 20 of 37 contigs; Fig. 3 and S6a). All *msg* genes identified were oriented towards one end of the contig, *i.e.* presumably towards the telomere (no telomeric repeats were identified for an unknown reason; Supplementary note 2). Except pseudogenes which were dispersed all over the subtelomeres, all members of family I were the closest to the end of their contig, *i.e.* proximal to the telomere (Fig. 3 and S6). By

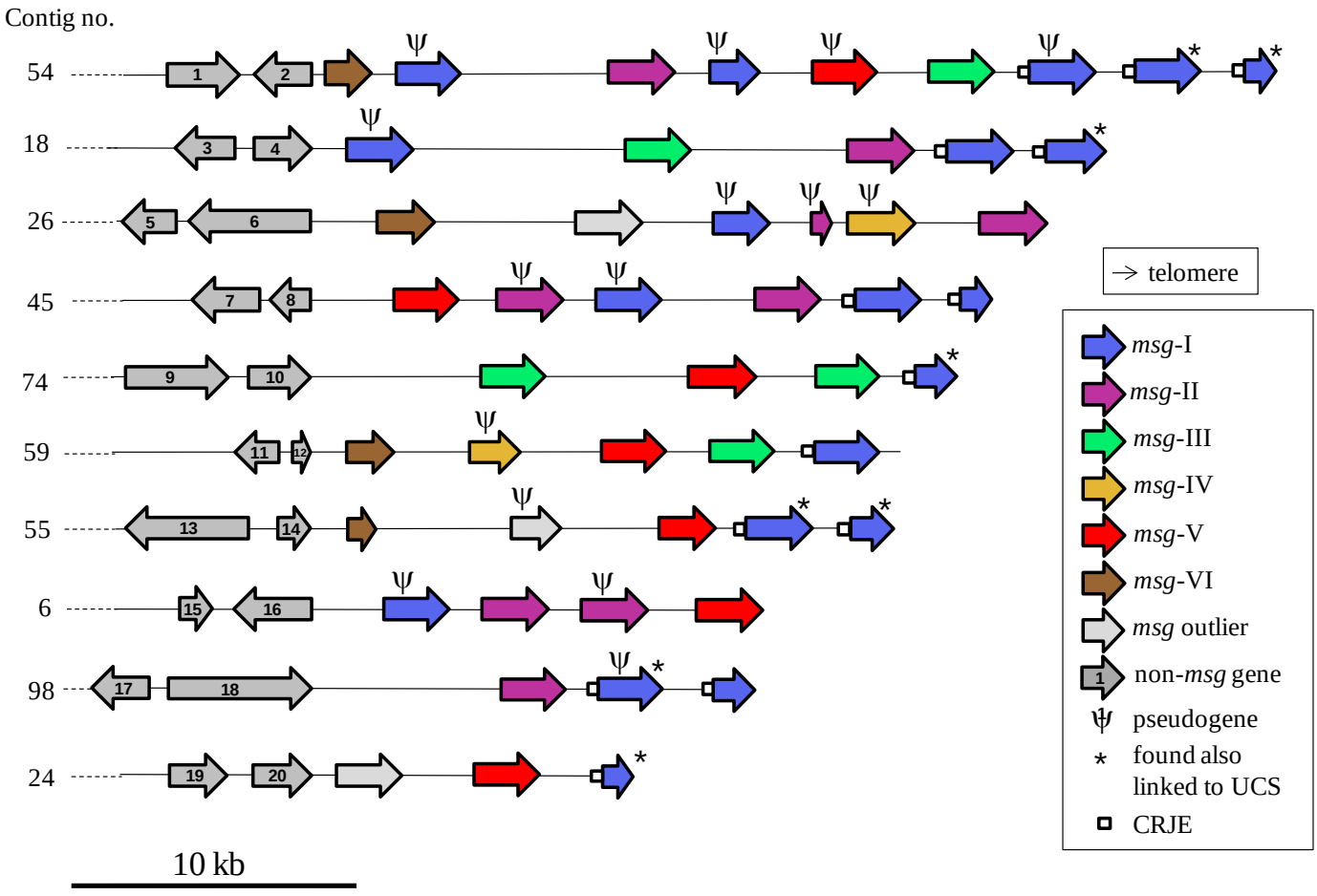

Fig. 3

Diagrams of ten representative *P. jirovecii* assembled subtelomeres. The other 27 assembled subtelomeres are shown in Figure S6. The attribution of the contigs to the chromosomes described by Ma et al (2016) using flanking non-msg genes is given in Table S3.

106 contrast, all members of family VI were the closest to the flanking non-*msg* genes present on
107 their contig, *i.e.* distal to the telomere. Members of the four remaining families were localized
108 centrally in the subtelomeres, between those of families I and VI. There were up to three *msg*-I
109 genes grouped at the end of 19 contigs. Members of the other five families did not show any
110 clear grouping pattern.
111
112 **Identification of the expression site of *msg*-I genes and of the genes linked to it**
113 Each infection by *P. jirovecii* is believed to involve a mixture of cells expressing different *msg*-I
114 genes under the control of the expression site, *i.e.* the UCS which is present at a single copy per
115 genome (Kutty et al. 2001). Consequently, the UCS was expected to be linked to different *msg*-I
116 genes in our DNA sample and thus cannot be unequivocally assembled, which plausibly explains
117 its absence from the PacBio assembly. A single UCS was retrieved from our DNA sample using
118 PCRs based on published sequences and it could be linked to one of the PacBio contigs
119 (Supplementary note 3). Consistently, this contig was linked to chromosome 1 which also carries
120 the UCS in the Ma et al (2016) assembly (Table S3). The UCS retrieved from our sample was
121 identical to that of Ma et al (2016), except few small changes not modifying the encoded protein
122 (Fig. S7). Interestingly, the CRJE sequence at the end of the UCS and beginning of each *msg*-I
123 gene presented an imperfect inverted repeat which was never pointed out so far (Fig. S7).
124 In order to identify the *msg*-I genes linked to the UCS in our sample, we amplified by PCR
125 the junction between these elements using one primer within the UCS and either (i) one primer
126 generic for many *msg*-I genes (Kutty et al. 2001), or (ii) one primer specific to a given *msg*-I
127 gene of the PacBio assembly (Supplementary note 4; Fig. 2a). Eighteen different *msg*-I genes
128 were found fused in frame to the UCS at the CRJE sequence, two being pseudogenes of the

129 family I with an upstream CRJE sequence, and four new *msg*-I sequences not present in the
130 PacBio assembly. The 14 *msg*-I genes found linked to the UCS which were present in the PacBio
131 assembly are identified in Figures 3 and S6 by asterisks. Three specific *msg*-I genes linked to the
132 UCS represented 74% of the subclones of the generic PCR analyzed, suggesting that sub-
133 populations of cells expressing given *msg*-I genes were of different sizes in our sample
134 (Supplementary note 4). These observations suggested that recombination between the CRJE
135 sequence of the UCS with that of different *msg*-I genes occurred at a high frequency in the single
136 *P. jirovecii* population studied here.
137
138 **Set of assembled subtelomeres**
139 The flanking non-*msg* genes allowed attributing 20 of our 37 contigs (Fig. 3 and S6a) to 15 of
140 the 20 full-length chromosomes described by Ma et al (2016) because they were also present in
141 the latter assembly (Table S3). All the remaining 17 contigs without flanking non-*msg* genes
142 (Fig. S6b) could have been assembled from the same subtelomeres as other contigs. Thus, we
143 assembled at least 20 subtelomeres out of the 40 potentially present in each cell. Given the
144 presence of a large number of subpopulations expressing different *msg*-I genes in our sample, the
145 set of subtelomeres present in each cell varied considerably. It is likely that the set we assembled
146 corresponded to a core of subtelomeres which was present in a majority of cells of the population
147 so that it could be assembled unequivocally.
148
149 **Recombination between *msg* genes**
150 Evidence of recombination events between *msg*-I genes was previously provided (Kutty et al.
151 2008). We investigated this issue among the different *msg* families using three different

numerical methods: two allowing analyses of large sets of genes for screening, and one analyzing only four genes at a time for more sensitive analysis. Two to 18 potential mosaic genes and their putative parent genes were detected within each family I to IV, involving sometimes partial or pseudogenes (Fig. 4; Table 2). On the other hand, only one potential mosaic gene was identified in family V and none in family VI ($P = 0.06$). Eight of the 30 mosaic genes detected shared with one parent a perfectly identical fragment of ca. 100 to 1000 bps, often close to the site of the predicted recombination events (Fig. 4b and S8). These latter cases suggested very recent recombination events. The putative parent genes of mosaic genes were randomly distributed among the two sub-clades of family I, suggesting that this family must be considered as a single entity (Supplementary note 5).

One to four potential recombination events per mosaic gene were generally identified using the two screening methods. These events were most often confirmed by the more sensitive method which, however, detected many other potential recombination events (Fig. 4 and S8). Consistent with the single mosaic gene detected in families V and VI, the frequency of recombination events appeared lower in these families than in the others (Fig. S9). This correlated with an average pairwise identity lower within each of these two families than within the others (45-66 versus 71-83%, Table 1). The predicted sites of the recombinations reported by all three methods were distributed randomly along the *msg* genes for all families, and did not contain any specific DNA sequence motifs (Fig. 4, S8, and S9). This suggested homologous rather than site-specific recombination events.

In contrast, we were unable to detect recombination events between different *msg* families, even using the more sensitive method (Fig. S10).

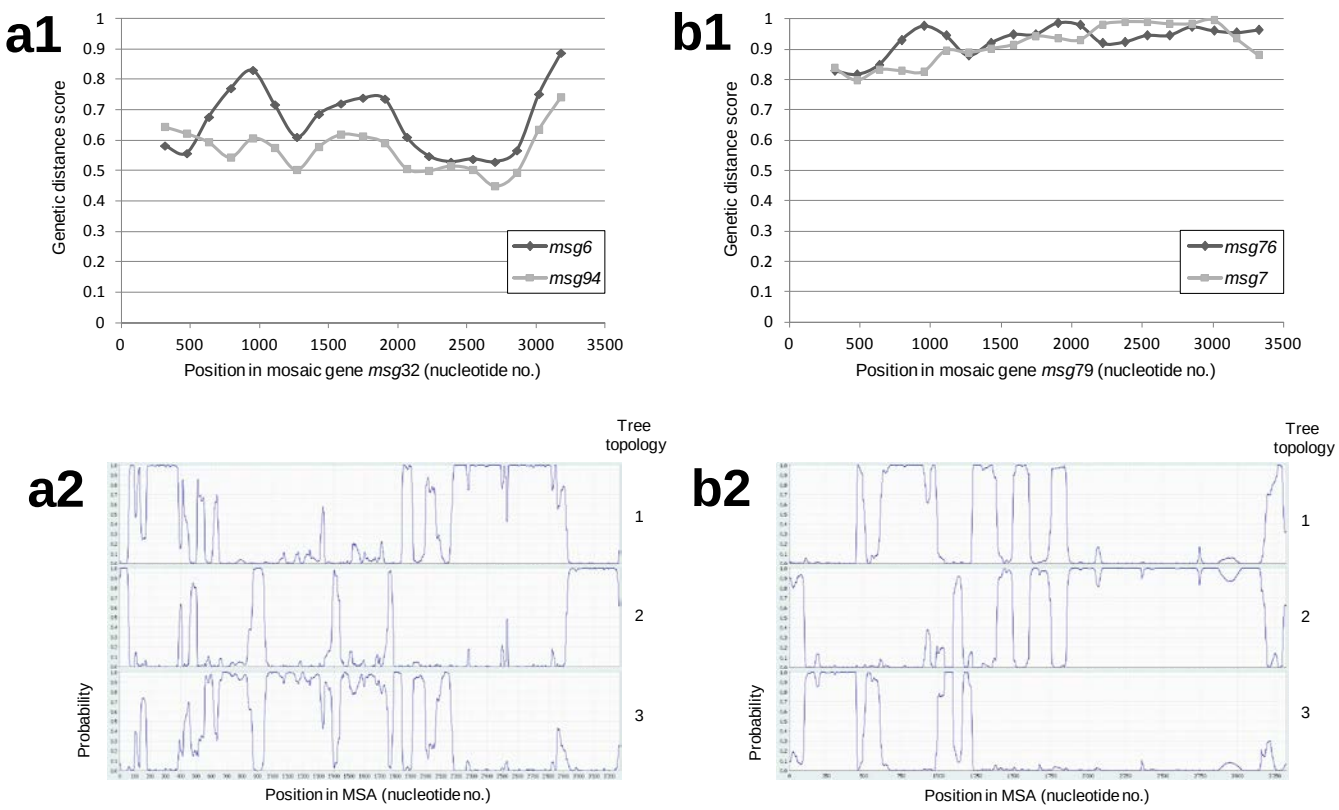

Fig. 4

Examples of detection of potential mosaic genes. (**a**) Mosaic gene *msg*32. (**a1**) The set of 11 full-length *msg*-I genes was analyzed using the Recombination Analysis Tool. This method measures genetic distances in windows sliding along the MSA. The genetic distance scores of the putative parent genes at the middle of each window are plotted against the position in the mosaic gene. The predicted recombination site is at position ca. 600, at the cross-over of the curves. The second screening method Bellerophon, which is based on a similar analysis, identified a recombination event at position 392. (**a2**) Analysis of the mosaic gene *msg*32 with its putative

(Legend Fig. 4 continued)

parent genes together with the randomly chosen *msg*84 of the same family using the more sensitive method TOPALi based on the Hidden Markov Model. This method analyses only four sequences at a time and calculates the probabilities of the three possible tree topologies at each residue of the MSA. A recombination event is also detected at position ca. 400-600, but several other recombination events are predicted. (**b**) Mosaic gene *msg*79. This gene shares an almost identical fragment of 947 bps with its putative parent *msg*7 (see alignment in Fig. S8c). (**b1**) The set of 11 full-length *msg*-II genes was analyzed using the Recombination Analysis Tool. The predicted recombination sites are at positions ca. 400, 1300, 2100, and 3100. The Bellerophon method did not identify this mosaic gene. (**b2**) Analysis of the mosaic gene *msg*79 with its putative parent genes together with the randomly chosen *msg*85 of the same family using TOPALi based on the Hidden Markov Model. Recombination events are also detected at positions ca. 400, 1500, and 3100, but not at 2100.

Table 2. Potential mosaic genes detected within each *msg* family [a].

	No. *msg* genes					No. potential *msg* mosaic genes				
msg family	Full-length	Partial	Pseudo	Total	Non-mosaic [b]	Full-length [c]	Partial	Pseudo [d]	Total [b]	% mosaic
I	11	16	16	43	25	8	1	9	18	42
II	11	3	4	18	13	4	1	0	5	28
III	7	2	1	10	6	3	0	1	4	40
IV	6	1	2	9	7	1	0	1	2	22
V [e]	8	6	1	15	14	1	0	0	1	7
VI [e]	6	1	0	7	7	0	0	0	0	0

[a] Detected using the Recombination Analysis Tool and / or Bellerophon bioinformatics screening methods among three different sets of genes of each *msg* family: full-length, full-length plus partial genes, full-length plus pseudogenes.

[b] The number of potential mosaic genes among the *msg* families was almost significantly different (P = 0.06, Chi-square test).

[c] Six full-length mosaic genes were detected twice but with different pairs of putative full-length parent genes according to the set of genes analysed (four, one, one of respectively family I, II, III). One mosaic gene of family I was detected twice: once with one full-length gene and one pseudogene as parents, and once with two partial genes as parents. All ten remaining were detected once with a pair of full-length parents.

[d] Six mosaic pseudogenes of family I had two pseudogenes as parents. Two of family I had one full-length gene and one pseudogene as parents. The three remaining had a pair of full-length parents.

[e] Several potential recombination events were detected for these two families using the more sensitive method TOPALi based on the Hidden Markov Model (Fig. S9).

Comparison to the *msg* superfamily previously proposed

The 146 *P. jirovecii msg* genes larger than 1.6kb reported by Ma et al (2016), out of a total of 179, were added into our DNA phylogenetic tree. They all clustered within our families, except 11 outliers (Fig. S11). The correspondence between the two sets of families is given in Table 1. The comparison of the two studies is detailed in the Supplementary note 6.

Discussion

Antigenic surface variation plays a crucial role in escaping the human immune system and adhering to host cells for important microbial pathogens. In the present study, we unravelled the mechanisms used by the fungus *P. jirovecii* for this purpose. Our observations show that its surface glycoproteins diversified during the evolution into a superfamily including six families each with its own structure, function, independent mosaicism, and expression mode.

Structure and function of Msg glycoproteins

Proteins of Msg family I were previously demonstrated to adhere human epithelial cell through binding to fibronectin and vitronectin (Pottratz et al. 1991; Limper et al. 1993). The ST-rich regions present in *P. jirovecii* Msg glycoproteins except those of family IV are sites of oxygen-linked glycosylation commonly involved in cell to cell adhesion (Dranginis et al. 2007). Moreover, most of these glycoproteins were predicted to be adhesins (Supplementary note 7). Consistently, their structure fits the model of modular organization of fungal adhesins with ST-rich regions at the C-terminus and a ligand binding domain at the N-terminus (Dranginis et al. 2007; Linder and Gustafsson 2008). Linder and Gustafsson (2008) proposed that, in addition to their role in adhesion, the oxygen-linked glycosylations of the ST-rich region confer rigidity to the protein in order to present outward the ligand domain. Thus, the N-terminus regions of the *P. jirovecii* adhesins may correspond to ligand binding domains. The fate and function of the glycoproteins of family IV remain enigmatic since they lack the ST-rich region, are only weakly predicted as adhesins (Supplementary note 7), and may not be attached to the cell wall in absence of a GPI anchor signal. The conserved leucines separated by two to six residues present in all *msg* families are similar to leucine zipper motifs which are often involved in protein-protein non-specific binding and protein dimerisation (Hakoshima 2005). This latter function is

also carried out by the PE-rich region present in *msg* family V and VI (Williamson 1994). The conserved coiled-coil domains discovered in Msg families I to III are often involved in the formation heteromultimers and protein complexes (Strauss and Keller 2008; Hitchcock-DeGregori and Barua 2017). The unstructured regions at the C-terminus present in four Msg families are not informative because these regions can have several different functions (Best 2017). These observations suggest that the Msg adhesins may form homo- or hetero-oligomers at the cell surface, possibly implying a further level of antigen variation which has never been envisaged so far.

Mosaicism of *msg* genes

Our observations suggest that a continuous and random creation of mosaic genes by homologous recombinations occurs mostly, if not exclusively, within each *msg* family. Very interestingly within the scope of protein annotation, this mechanism permits by itself to define the members of a protein family without having to rely upon the cutting of a phylogenetic tree at an arbitrary height. The frequency of these recombinations remains to be quantified precisely, but is likely to be reduced in *msg* families V and VI. The genetic mechanisms involved in the creation of mosaic genes may include a single homologous recombination leading to a telomere exchange, or two homologous recombinations leading to a gene fragment conversion or exchange (models are shown in Fig. S12a). Such recombinations could also produce partial genes if they occur between homologous regions which are not located at the same position along the recombining genes. Our results suggest that this is rare because we identified only three partial *msg* genes out of 113. This conclusion is also consistent with the fact that different motifs are conserved along the sequence of the Msg proteins of each family. Our data suggest that pseudogenes might also be involved in the generation of mosaic genes, and thus might constitute a reservoir of sequences

that can be integrated into functional antigens. The pseudogenes may result from accumulation of mutations in absence of expression and thus of selective pressure. This phenomenon could be enhanced by mutation and recombination rates within the subtelomeric gene families higher than in the rest of the genome (Barry et al. 2003). The presence of the pseudogenes in the subtelomeres might simply correspond to the state between their birth and their future decay. However, they could also be maintained within the subtelomeres through indirect selective pressure because of their role as reservoir of sequences for the creation of mosaic genes.

Mutually exclusive expression of *msg*-I genes

Our conclusions concerning the mutually exclusive expression of the *msg*-I genes are in agreement with previous studies, but bring support for the involvement of telomere exchange which has been previously hypothesized (Sunkin and Stringer 1996). The exchange of the single expressed gene by recombination at the CRJE sequences might be facilitated by the localization of the *msg*-I genes closest to the telomeres because this may in turn facilitate telomere exchanges (a model is shown in Fig. S12b). These recombinations could be homologous in nature because the full identity over 33 bps might be sufficient as it is the case in fungal cousins (Hua et al. 1997). However, they could also be site-specific because the imperfect inverted repeat present in the CRJE is a common motif used by site-specific recombinases (Turan and Bode 2011). Up to three *msg*-I genes were present at the end of the subtelomeres. There is no reasons to exclude that transfer of more than one *msg*-I gene to the expression site at once also occurs, followed by polycistronic expression. The polypeptide produced could be then chopped by the endoprotease Kex1 at the end of each CRJE and each Msg-I anchored to the cell wall separately through its own GPI signal. Interestingly, we detected *msg*-I pseudogenes linked to the UCS using PCR in our sample. The cells expressing such truncated antigens may not be selected over time during

the infection because of their likely deficiency in adhesion to the host cells. They might constitute a cost inherent to such system of antigenic variation based on frequent recombination events.

Expression of *msg* families

RNAseq analyses suggested that the vast majority of the *msg* genes of all families were expressed in *P. carinii* and *P. murina* populations (Ma et al. 2016). As far as *P. jirovecii* is concerned, alignment of our previous RNAseq data (Cissé et al. 2012) with the subtelomeres assembled in the present study was compatible with the same conclusion, although the data were from different clinical isolates (results not shown). Expression of most *msg*-I genes at the population level is consistent with the numerous subpopulations of cells expressing different *msg*-I genes that we observed. As far as *msg* families II to VI are concerned, the RNAseq data are compatible with constitutive or temporally regulated expression of all genes in each cell driven by the promoter present upstream of each of these genes. However, they are also compatible with mutually exclusive or partially exclusive expression of these genes thanks to silencing of promoters, or through another unknown mechanism.

Model of expression of *msg* genes and cell surface structure

In absence of data at the single cell level which would unravel the mode of expression of *msg* genes, we propose a model of cellular expression of the *msg* families and cell surface structure (Fig. 5). This model is based on the working hypothesis that all *msg* genes except those of family I are expressed constitutively in both trophic forms and asci. The UCS is a strong promoter (Kutty et al. 2013), probably leading to a majority of a single isoform of adhesive Msg-I antigens on the cellular surface. This is consistent with the fact that Msg-I antigens are the most abundant

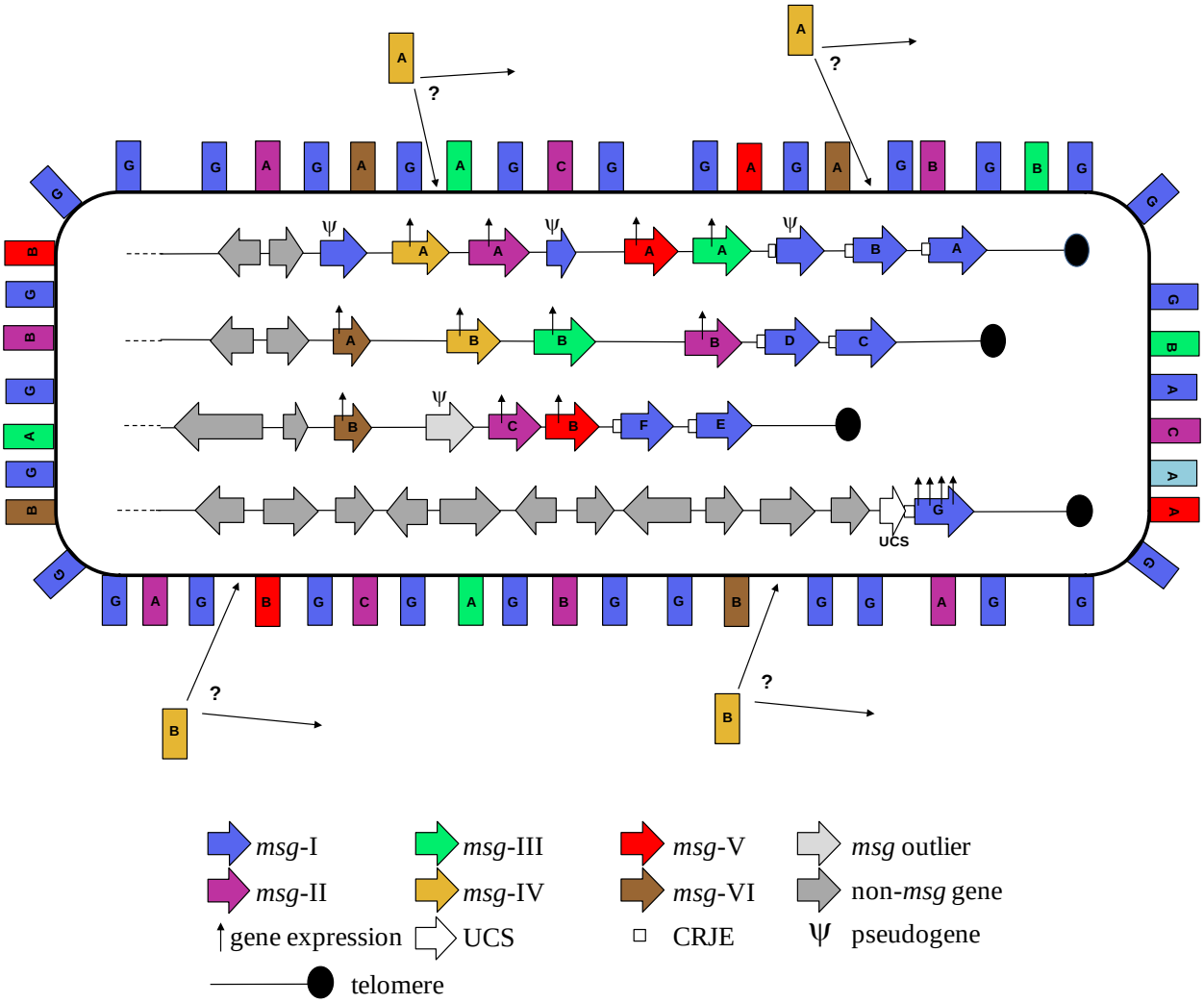

104
105

106

107

108 **Fig. 5**

109 Model of expression of *msg* genes and cell surface structure. The level of gene expression is

110 figured by the number of arrows. The different isoforms of each *msg* family are differentiated by

111 capital letters. The fate of the Msg-IV proteins remains to be determined (see text). The INT1

112 and other surface proteins are not figured.

113

proteins in *Pneumocystis* species. All the different isoforms of adhesive glycoproteins of the other families than family I present in the cell would be expressed and present on the cell surface at the same time. The surface of *P. carinii* trophic cells was shown to harbour also the protein INT1 participating to adhesion (Kottom et al. 2008). Recently, a transcription factor responsible for expression of (a) still unidentified adhesive surface protein(s) has been reported in *P. carinii* trophic cells (Kottom and Limper 2016). Genes encoding orthologs of these proteins are also present in *P. jirovecii* genome (results not shown). Moreover, Kottom and Limper (2016) mentioned that other uncharacterized genes which are important in binding to mammalian hosts are present in *P. carinii* genome. Thus, the structure of the cell surface of both trophic forms and asci is made of a complex mixture of different glycoproteins. The latter conclusion is valid whatever the mode of expression of families II to VI is in reality.

Strategy of antigenic variation

The exchange of the *msg*-I isoform expressed and the generation of new mosaic genes of all *msg* families would lead to a continuous segregation of subpopulations with a new mixture of glycoproteins at the cell surface. Thus, the strategy of the fungus would consist in the continuous generation of cells which are antigenically different. This strategy is further suggested by other characteristics of *Pneumocystis* spp. First, there is a high variability of the subtelomeres between *P. jirovecii* isolates[4] which is consistent with frequent subtelomeric recombinations. The subtelomeres of the isolate we studied here also differed greatly from those of the same chromosomes reported by Ma et al (2016) (Supplementary note 6). Second, sexuality could be obligatory in the cell cycle (Cushion and Stringer 2010; Hauser 2014) because most ectopic recombinations between subtelomeres occur during meiosis, within the bouquet of telomeres formed (Barry et al. 2003). The likely homothallic sexuality of *Pneumocystis* spp (Almeida et al.

2015) avoids the need to find a compatible partner and thus increases mating frequency, which is believed to favor genetic diversity (Roach and Heitman 2014). Moreover, the genetic diversity might be enhanced by mating between the numerous co-infecting strains which are generally present in *P. jirovecii* infections (Alanio et al. 2016). Third, the presence of several *msg* families may allow the formation of Msg hetero-oligomers that we envisage above, which would further enhance the cell surface complexity.

Strategies of antigenic variation in different human pathogens

The mechanisms and hypothesised strategy of antigenic variation unravelled here appear unique among human pathogens. *Candida glabrata* contain one subtelomeric family of ca. 20 adhesins (Deitsch et al. 2009). *Trypanosoma brucei* presents a large reservoir of sequences used to create mosaic genes of a single surface antigen family made of about a thousand of genes located in subtelomeres as well as on minichromosomes (Deitsch et al. 2009). In the latter organism, pseudogenes provide segments to mosaic functional antigens (Hall et al. 2013), a phenomenon which might also occur in *P. jirovecii*. *Plamsodium falciparum* harbours one subtelomeric antigen family of ca. 60 members (Deitsch et al. 2009). These three organisms present a single gene family subject to mutually exclusive expression involving silencing in several cases. Thus, their populations are homogenous antigenically but may vary over time when the expressed gene is exchanged. Such strategy might be imposed by sterile niches such as blood and urinary tract. This contrasts sharply with the putative strategy of antigenic variation of *P. jirovecii* consisting in the continuous production of a mixture of cells antigenically different. The latter strategy may be associated to the particular niche within lungs since it tolerates the presence of low abundant fungi as members of the natural lung microbiota. This strategy might allow presenting most cells as different organisms to the immune system and thus to be tolerated during colonisation. A

similar strategy might be used by *Candida albicans* living in non-sterile mucosal niches. Indeed, its unique adhesin family presents a high number of serine CUG codons which are ambiguously translated into serine or leucine, thus creating variability from individual genes (Rizzetto et al. 2015).

Trypanosoma and *Plasmodium* also differ from *Pneumocystis* spp in that they infect two different hosts rather than one. This undoubtedly exerts a different selective pressure on their antigenic variation system. The *Pneumocystis* spp differ considerably in their *msg* families (Ma et al. 2016), as well as in the fine structure of the Msg adhesins (Mei et al. 1998). It is likely that these differences are involved in the strict host species specificity of these fungi. Further work aiming at understanding the relation between structure and function of the different Msg glycoproteins is needed to further decipher both antigenic variation and host specificity of these fungi.

Methods

Bronchoalveolar lavage fluid specimens. Fresh BALFs positive for *P. jirovecii* using Methenamine-silver nitrate staining (Musto et al. 1982) were supplemented with 15% v/v glycerol, frozen in liquid Nitrogen, and stored at -80°C. Only those with more than one ml available and heavy fungal load were stored. Seventeen specimens were stored between 2012 and 2014, and used for the selection procedure described here below.

DNA extraction and identification of an infection with a single *P. jirovecii* strain. Genomic DNA was extracted from 0.2 to 0.4 ml of BALF specimen using QIAamp® DNA Mini kit (Qiagen), and resuspended in 50 µl of elution buffer. Four genomic regions were amplified by PCR from genomic DNA extracted as described previously (Hauser et al. 1997). Each PCR product was cloned into the plasmid pCR™4-TOPO using the TOPO TA cloning Kit for Sequencing (Life Technologies). Both strands of the insert of 15 clones for each genomic region were sequenced with M13 primers using the BigDye Terminator kit and the ABI Prism 3100 automated sequencer (both from PerkinElmer Biosystems). Among the 17 clinical specimens collected, only one generated identical sequences for all clones of all genomic regions. Since ca. 15 clones per genomic region were analyzed, a second eventual co-infecting strain in this specimen should not represent more than ca. 7% of the *P. jirovecii* population. This specimen was selected for all experiments performed in the present study. It was from a HIV-infected patient.

Enrichment in *P. jirovecii* DNA and random amplification. The DNA of the selected specimen was enriched in *P. jirovecii* DNA using the NEBNext® Microbiome DNA Enrichment

Kit based on the absence of CpG methylation (Biolabs), purified by ethanol precipitation in presence of 10 µg glycogen (Thermo Fisher Scientific), and resuspended in 50 µl of 1X TE Buffer. This enrichment raised the proportion of *P. jirovecii* DNA from a few percent to ca. 55% as determined *a posteriori* by high throughput sequencing. Because only small amounts of DNA are recoverable from a clinical specimen and in absence of an *in vitro* culture system, sufficient amount of DNA for high throughput PacBio sequencing was obtained by random amplification. Five µl of DNA was randomly amplified in a 50 µl reaction using the Illustra GenomiPhi HY DNA Amplification Kit (GE Healthcare). This amplification proved to create artificial molecules made of inverted repeats of several kb which were revealed by PacBio sequencing. The reads from these molecules were eliminated by bioinformatics (see below). DNA was then purified using QIAamp® DNA blood mini kit (Qiagen) followed by ethanol precipitation in presence of 10 µg glycogen. Amplified DNA fragments were sized (mean 8.6 kb) and quantified using Fragment Analyzer™ (Advanced Analytical).

High throughput PacBio sequencing. Five µg of amplified DNA were used to prepare a SMRTbell library with the PacBio SMRTbell Template Prep Kit 1 according to the manufacturer's recommendations (Pacific Biosciences). The resulting library was size selected on a BluePippin system (Sage Science) for molecules larger than 5 kb. The recovered library was sequenced on one SMRT cell with P6/C4 chemistry and MagBeads on a PacBio RSII system (Pacific Biosciences) at 240 min movie length.

Read filtering and *P. jirovecii* genome assembly. The flow chart of the filtering and assembly procedure is shown in Figure S13a and the details for each step are described here. PacBio sub-reads were extracted from the raw h5-files using DEXTRACTOR

(https://github.com/thegenemyers/DEXTRACTOR/). The average length of the extracted sub-reads was 5.2 kb with a maximum of 42 kb. We removed human derived reads by mapping them against the human reference genome using blasr (smrtpipe2.3, cut-off: corrected score < 55000). Reverse-complementary artificial reads created by the random amplification were next filtered out (cut-off:match length >=1000 bps) after mapping them onto themselves using DALIGNER (https://github.com/thegenemyers/DALIGNER/)(V1.0, options:-A -I). The cleaned reads were assembled using the tool FALCON (Chin et al. 2016)(V0.2, options: length_cutoff=8000m length_cutoff_pr=1000). PacBio reads were re-mapped onto the assembly using BLASR and used to evaluate and flag remaining human contigs. Human derived contigs were subsequently removed. A total of 2.2 Gb of *P. jirovecii* DNA sequences corresponding to a 200-fold coverage of the genome were gathered. The assembly was polished to remove residual PacBio errors using Quiver (Chin et al. 2013)(smrtpipe2.3, 5 iterations). The final polished genome assembly included 8.1 Mb in 219 gap-free contigs ranging from 234 bps to 386 kb with a NG50 of 108Kb, and 57% of the genome in 28 contigs lager than 100 kb. The *P. jirovecii* PacBio assembly obtained in the present study covered 96% of that we previously obtained using other sequencing methods[6], and contained ca. 0.5 Mbp of subtelomeric sequences. The combination of both our assemblies covered 97% the assembly of Ma et al (2016). Controls consisting in PCR amplification of specific subtelomeric regions from the same DNA sample confirmed the accuracy of the nucleotide sequence of the polished PacBio assembly, although few errors in repetitive homopolymer regions were detected (Supplementary note 8).

Gene predictions and *msg* annotations. Genes were predicted on the assembly using Augustus (Stanke et al. 2006)(version 2.5.5) and a specifically trained model for *Pneumocystis* (Cissé et al. 2012). In order to detect novel and more distant homologous *msg* genes in the assembly, we

chose a generalized profile based approach (Bucher and Bairoc 1994)(Fig. S13b). A DNA profile was generated based on a previously described *msg* gene in *P. carinii* (Wada and Nakamura 1996)(GenBank D82031.1) and a protein profile based on Msg-Rucl 21 (European Nucleotide Archive ABQ51002.1) using a Smith-Waterman-Algorithm (Smith and Waterman 1981). The profiles were calibrated against the scrambled genome (window approach, size=60). Using pfsearchV3 (Schuepbach et al. 2013), the assembled genome was searched for homologues matches with the DNA profile. Curated matches were extracted and aligned against each other using MAFFT (Katoh and Standley 2013)(version 7.305). After manual curation and trimming, the alignments were divided in five groups based on neighbourhood joining (% identity) using Jalview (Waterhouse eta l. 2009)(v2.8.1). One representative candidate per group was selected and a new profile based on its sequence generated and calibrated as described here above. These DNA *msg* profiles were used to find and annotate a first set of 75 *msg* genes in the assembly. A combination of Blastx, genewise, in-house tools, and manual curation was applied using the protein Msg profile to extend and correct these annotations to the set of 113 *msg* genes analysed in the present study. The *msg* genes reported here were all manually curated with respect to their start, stop and intron coordinates.

Construction of phylogenetic trees. For the DNA and protein based phylogenetic analysis, the CDS for each annotated *msg* gene was manually corrected (up to five corrections), extracted, and translated into its protein sequence. Both CDS and protein sequences were aligned against each other using MAFFT (Katoh and Standley 2013)(mafft-linsi –genafpair), and the multiple sequence alignment used to infer a phylogenetic tree with RAxML (Stamatakis 2014)(PROTGAMMAGTR for proteins and with GTRGAMMA for CDS, 1000 bootstraps). The *msg* genes of family V were defined as out-group and the final tree rooted. Proteins were further

classified using JACOP (Sperisen and Pagni 2005)(http://myhits.isb-sib.ch/cgi-bin/jacop/). In order to add pseudogenes and published *msg* genes from Ma et al (2016) equal or exceeding 1.6 kb, we injected the new sequences into the prior DNA-based multiple-alignment using MAFFT (Katoh and Standley 2013)(--addfull). They were added to the original tree using the evolutionary placement algorithm (EPA) from RAxML. These trees were converted into a compatible format with the tool guppy from the pplacer suite (Matsen et al. 2010) (v1.1alpha14, tog). Genes with an exon smaller than 1.6 kb were added to the original DNA-based multiple-alignment using MAFFT (Katoh and Standley 2013)(--addfragments). The alignment was trimmed and re-aligned using MAFFT (Katoh and Standley 2013). A new tree was then build with RAxML (GTRGAMMA, 1000 bootstraps). All trees were analyzed and visualized using R (R Core Team 2013)(3.3.2) and GGTREE (Yu et al. 2017)(v1.6.9).

Gene and protein sequences analyses. Alignments of full-length gene or protein sequences were carried out using MAFFT (Katoh and Standley 2013). Canonical TATA box and Cap signal (Bucher 1990), as well as canonical donor and acceptor sequences of *Pneumocystis* introns (Thomas et al. 1999; Slaven et al. 2006), were identified by visual inspection of the alignments and sequences of the genes. Signal peptide and GPI anchor signal were identified using respectively Phobius (Käll et al. 2004)(http://phobius.sbc.su.se/) and GPI-SOM (Frankhauser and Mäser 2005)(http://gpi.unibe.ch/) with default settings. Canonical potential sites NXS/T of Nitrogen-linked glycosylation (Linder and Gustafsson 2008) were identified by visual inspection. Conserved domains were searched using Multiple Expectation–Maximization for Motif Elicitation (Bailey and Elkan 1994)(MEME, http://meme-suite.org/tools/meme). MEME analysis of the 49 full-length Msg proteins of all families except outliers was carried out using default settings, except minimum and maximum motif width of respectively 50 and 100 residues, any

number of sites per sequence option, and maximum of 13 motifs searched. HMMER (Finn et al. 2011)(biosequence analysis using profile hidden Markov models, http://www.ebi.ac.uk/Tools/hmmer/search/hmmscan) was used with default settings on full-length proteins for the following embedded predictions: Pfam, unstructured regions (Intrinsically Unstructured Proteins, IUPRED), and coiled-coil motifs (Ncoils predictor). Pairwise identities between full-length *msg* genes and Msg proteins were calculated using the multi-way alignment type of Clone Manager 9 professional edition software.

Search for potential mosaic genes. Two screening methods were first used: Recombination Analysis tool (Etherington et al. 2005)(RAT, http://cbr.jic.ac.uk/dicks/software/RAT/) and Bellerophon (Huber et al. 2004)(http://comp-bio.anu.edu.au/bellerophon/bellerophon.pl). MAFFT (Katoh and Standley 2013) alignments of various set of genes were analysed with both methods. RAT was used with default settings, *i.e.* using windows of one tenth of the length of the alignment and increment size equal to half of the window size. Bellerophon was used with default settings, *i.e.* windows of 300 bps and Huber-Hugenholtz correction. RAT can detect several recombination events whereas Bellerophon reports a single one per mosaic gene. The more sensitive method TOPALi v2.5 (Milne et al. 2004)(http://www.topali.org/) which is based on a Hidden Markov Model (HMM) was then applied on the potential mosaic genes and its putative parent genes detected with the two screening methods. These three genes were aligned using MAFFT (Katoh and Standley 2013) with an additional gene chosen randomly in the same *msg* family since TOPALi requires four genes in input. The efficacy of the three methods to detect mosaic genes was assessed by the analysis of artificial chimera produced *in silico* with related genes, as well as with sets of orthologous genes from different fungal species (results not shown). Only the RAT method is suitable for the search of recombination events among proteins.

The vast majority of the events detected at the protein level corresponded to those detected at the DNA level (results not shown).

PCR amplification and sequencing. PCRs were performed in a final volume of 20 µl with 0.35 U of High Fidelity Expand polymerase (Roche Diagnostics), using the buffer provided, each dNTP at a final concentration of 200 µM, and each primer at 0.4 µM. PCR conditions included an initial denaturation step of 3 min at 94°C, followed by 35 cycles consisting of 30 s at 94°C, 30 s at the annealing temperature, and 1 min per kb to be amplified at 72°C. The reaction ended with 5 min of extension at 72°C. The annealing temperature and the $MgCl_2$ concentration were optimized for each set of primers and ranged from 51 to 60°C and from 3 to 6 mM, respectively. Sequencing both strands of the PCR products was performed with the two primers used for PCR amplification, as well as the Big Dye Terminator DNA sequencing kit and ABI PRISM 3100 automated sequencer (both from Perkin-Elmer Biosystems).

Ethics

The protocol was approved by the institutional review board (Commission cantonale d'éthique de la recherche sur l'être humain). All patients provided an informed written consent which was part of procedure for the admittance in the hospital. This consent was documented by the fact that they did not ask their samples not to be used for research. The samples were treated anonymously.

Availability of data and materials

PacBio raw reads (accession SRR5533719) and PacBio assembly (accession NJFV00000000) have been deposited at DDBJ/ENA/GenBank linked to BioProject PRJNA382815 and

BioSample SAMN06733346. The version of the PacBio assembly described in this paper is version NJFV01000000.

Acknowledgments

Computations were performed at the Vital-IT Center for High-Performance Computing of the Swiss Institute of Bioinformatics (http://www.vital-it.ch). We thank Michel Monod, Dominique Sanglard, and Laurent Keller for critical reading.

Supplementary information

The table of contents of the Supplementary information is in Additional file 2.docx, together with supplementary notes and figures. Supplementary Tables are in Additional file 1.docx.

Funding

This work was supported by the Swiss National Science Foundation, grant 310030_146135 to P.M.H. and M.P. This Foundation had not role in any steps of the study.

Authors' contributions

P.M.H. and M.P designed the study. S.R. and A.L. collected and prepared the samples, and carried out the laboratory experiments. K.M. collected and prepared samples. E.S.-S. performed genome assembly. E.S.-S. and P.M.H. performed bioinformatics analyses. E.S.-S., P.M.H., S.R., A.L., and M.P. analysed the data. P.M.H., E.S.-S., and M.P. wrote the manuscript.

Competing interests

The authors declare no competing interests.

References

Alanio A, Gits-Muselli M, Mercier-Delarue S, Dromer F, Bretagne S. 2016. Diversity of *Pneumocystis jirovecii* during infection revealed by ultra-deep pyrosequencing. *Front Microbiol* **7:** 733.

Almeida JMGCF, Cissé OH, Fonseca Á, Pagni M, Hauser PM. 2015. Comparative Genomics suggests Primary Homothallism of *Pneumocystis* species. *Mbio* **6:** e02250-e02214.

Bailey TL, Elkan C. 1994. Fitting a mixture model by expectation maximization to discover motifs in biopolymers. *Proc Sec Int Conf Int Syst Mol Biol* 28-36 (AAAI Press, Menlo Park, California).

Barry JD, Ginger ML, Burton P, McCulloch R. 2003. Why are parasite contingency genes often associated with telomeres? *Int J Parasit* **33:** 29-45.

Best RB. 2017. Computational and theoretical advances in studies of intrinsically disordered proteins. *Curr Opin Struct Biol* **42:** 147-154.

Brown GD, Denning DW, Gow NAR, Levitz SM, Netea MG, White TC. et al. 2012. Hidden killers: human fungal infections. *Sci Transl Med* **4:** 165rv13.

Bucher P. 1990. Weight matrix descriptions of four eukaryotic RNA polymerase II promoter elements derived from 502 unrelated promoter sequences. *J Mol Biol* **212:** 563-578.

Bucher P, Bairoc AA. 1994. Generalized profile syntax for biomolecular sequence motifs and its function in automatic sequence interpretation. *Proc Int Conf Intell Syst Mol Biol* **2:** 53-61.

Chin CS, Peluso P, Sedlazeck FJ, Nattestad M, Concepcion GT, Clum A, et al. 2016. Phased diploid genome assembly with single-molecule real-time sequencing. *Nat Meth* **13:** 1050-1054.

390 Chin CS, Alexander DH, Marks P, Klammer AA, Drake J, Heiner C, et al. 2013. Nonhybrid,
391 finished microbial genome assemblies from long-read SMRT sequencing data. *Nat Meth* **10:**
392 563-569.
393 Cissé OH, Pagni M, Hauser PM. 2012. *De novo* assembly of the *Pneumocystis jirovecii* genome
394 from a single bronchoalveolar lavage fluid specimen from a patient. *MBio* **4:** e00428-00412.
395 Cushion MT, Smulian AG, Slaven BE, Sesterhenn T, Arnold J, Staben C, et al. 2007.
396 Transcriptome of *Pneumocystis carinii* during fulminate infection: carbohydrate metabolism
397 and the concept of a compatible parasite. *PLoS ONE* **2:** e423.
398 Cushion MT, Stringer JR. 2010. Stealth and opportunism: alternative lifestyles of species in the
399 fungal genus *Pneumocystis*. *Annu Rev Microbiol* **64:** 431-452.
400 Deitsch KW, Lukehart SA, Stringer JR. 2009. Common strategies for antigenic variation by
401 bacterial, fungal and protozoan pathogens. *Nat Rev* **7:** 493-503.
402 Dranginis AM, Rauceo JM, Coronado JE, Lipke PN. 2007. A Biochemical Guide to Yeast
403 Adhesins: Glycoproteins for Social and Antisocial Occasions. *Microbiol Mol Biol Rev* **71:**
404 282-294.
405 Etherington GJ, Dicks J, Roberts IN. 2005. Recombination Analysis Tool (RAT): a program for
406 the high-throughput detection of recombination. *Bioinfo* **21:** 278-281.
407 Fankhauser N, Mäser P. 2005. Identification of GPI anchor attachment signals by a Kohonen
408 self-organizing map. *Bioinfo* **21:** 1846-1852.
409 Finn RD, Clements J, Eddy SR. 2011. HMMER web server: interactive sequence similarity
410 searching. *Nucl Ac Res* **39:** W29-W37.
411 Hakoshima T. 2005. Leucine Zippers. eLS.
412 Hall JPJ, Wang H, Barry JD. 2013. Mosaic *VSGs* and the scale of *Trypanosoma brucei* antigenic
413 variation. *PLoS Pathog* **9:** e1003502.

414 Hauser PM. 2014. Genomic insights into the fungal pathogens of the genus *Pneumocystis*:
415 obligate biotrophs of humans and other mammals. *PLoS Pathog* **10:** e1004425.
416 Hauser PM, Francioli P, Bille J, Telenti A, Blanc DS. 1997. Typing of *Pneumocystis carinii* f.
417 sp. *hominis* by single-strand conformation polymorphism of four genomic regions. *J Clin*
418 *Microbiol* **35:** 3086-3091.
419 Hitchcock-DeGregori SE, Barua B. 2017. Tropomyosin structure, function, and interactions: a
420 dynamic regulator. *Sub Biochem* **82:** 253-264.
421 Hua SB, Qiu M, Chan E, Zhu L, Luo Y. 1997. Minimum length of sequence homology required
422 for *in vivo* cloning by homologous recombination in yeast. *Plasmid* **38:** 91-96.
423 Huber T, Faulkner G, Hugenholtz P. Bellerophon: a program to detect chimeric sequences in
424 multiple sequence alignments. Bioinfo. 2004;20:2317-9.
425 Käll L, Krogh A, Sonnhammer ELL. 2004. A Combined Transmembrane Topology and Signal
426 Peptide Prediction Method. *J Mol Biol* **338:** 1027-1036.
427 Katoh K, Standley DM. 2013. MAFFT multiple sequence alignment software version 7:
428 improvements in performance and usability. *Mol Biol Evol* **30:** 772-780.
429 Keely SP, Renauld H, Wakefield AE, Cushion MT, Smulian AG, Fosker N, et al. 2005. Gene
430 arrays at *Pneumocystis carinii* telomeres. *Genetics* **170:**1589–1600.
431 Keely SP, Stringer, JR. 2009. Complexity of the MSG gene family of *Pneumocystis carinii*.
432 *BMC Gen* **10:** 367.
433 Kottom TJ1, Kennedy CC, Limper AH. 2008. *Pneumocystis PCINT1*, a molecule with integrin-
434 like features that mediates organism adhesion to fibronectin. *Mol Microbiol* 67: 747-761.
435 Kottom TJ, Limper AH. 2016. Evidence for a *Pneumocystis carinii* Flo8-like transcription
436 factor: insights into organism adhesion. *Med Microbiol Immunol* **205:** 73-84.

437 Kutty G, Ma L, Kovacs JA. 2001. Characterization of the expression site of the major surface
438 glycoprotein of human-derived *Pneumocystis carinii*. *Mol Microbiol* **42:** 183-193.
439 Kutty G, Shroff R, Kovacs JA. 2013. Characterization of *Pneumocystis* major surface
440 glycoprotein gene (*msg*) promoter activity in *Saccharomyces cerevisiae*. *Euk Cell* **12:** 1349-
441 1355.
442 Kutty G, Maldarelli F, Achaz G, Kovacs JA. 2008. Variation in the major surface glycoprotein
443 genes in *Pneumocystis jirovecii*. *J Infect Dis* **198:** 741-749.
444 Linder T, Gustafsson CM. 2008. Molecular phylogenetics of ascomycotal adhesins—a novel
445 family of putative cell-surface adhesive proteins in fission yeasts. *Fung Gen Biol* **45:** 485-
446 497.
447 Limper AH, Standing JE, Ho¡man OA, Castro M, Neese, LW. 1993. Vitronectin binds to
448 *Pneumocystis carinii* and mediates organism attachment to cultured lung epithelial cells.
449 *Infect Immun* **61:** 4302-4309.
450 Ma L, Chen Z, Wei Huang D, Kutty G, Ishihara M, Wang H, et al. 2016. Genome analysis of
451 three *Pneumocystis* species reveals adaptation mechanisms to life exclusively in mammalian
452 hosts. *Nat com* **7:** 10740.
453 Ma L, Kutty G, Jia Q, Imamichi H, Huang L, Atzori C, et al. 2002. Analysis of variation in
454 tandem repeats in the intron of the major surface glycoprotein expression site of the human
455 form of *Pneumocystis carinii*. *J Infect Dis* **186:** 1547-1554.
456 Matsen FA, Kodner RB, Armbrust, EV. 2010. pplacer: linear time maximum-likelihood and
457 Bayesian phylogenetic placement of sequences onto a fixed reference tree. *BMC Bioinfo* **11:**
458 538.

Mei Q, Turner RE, Sorial V, Klivington D, Angus CW, Kovacs JA. 1998. Characterization of major surface glycoprotein genes of human *Pneumocystis carinii* and high-level expression of a conserved region. *Infect Immun* **66:** 4268-4273.

Milne I, Wright F, Rowe G, Marshal DF., Husmeier D, McGuire G. 2004. TOPALi: software for automatic identification of recombinant sequences within DNA multiple alignments. *Bioinfo* **20:** 1806-1807.

Musto L, Flanigan M, Elbadawi A. 1982. Ten-minute silver stain for *Pneumocystis carinii* and fungi in tissue sections. *Arch Pathol Lab Med* **106:** 292-294.

Pottratz ST, Paulsrud J, Smith JS, Martin WJ II. 1991. *Pneumocystis carinii* attachment to cultured lung cells by *Pneumocystis* gp 120, a fibronectin binding protein. *J Clin Invest* **88:** 403-407.

R Core Team. 2013. R: a language and environment for statistical computing. R Foundation for Statistical Computing, Vienna, Austria. URL http://www.R-project.org/.

Ramana J, Gupta, D. FaaPred: 2010. A SVM-based prediction method for fungal adhesins and adhesin-like proteins. *PLoS ONE* **5:** e9695.

Rizzetto L, Weil T, Cavalieri D. 2015. Systems level dissection of *Candida* recognition by dectins: a matter of fungal morphology and site of infection. *Pathog* **4:** 639-661.

Roach KC, Heitman J. 2014. Unisexual reproduction reverses Muller's ratchet. *Genetics* **198:** 1059-1069.

Schuepbach T, Pagni M, Bridge A, Bouqueleret L, Xenarios I, Cerutti L. 2013. pfsearchV3: a code acceleration and heuristic to search PROSITE profiles. *Bioinfo* **29:** 1215-1217.

Slaven BE, Porollo A, Sesterhenn T, Smulian AG, Cushion MT, Meller J. 2006. Large-scale characterization of introns in the *Pneumocystis carinii* genome. *J Eukar Microbiol* **53:** S151-153.

Smith TF, Waterman MS. 1981. Identification of common molecular subsequencees. *J Mol Biol* **147:** 195-197.

Sperisen P, Pagni M. 2005. JACOP: a simple and robust method for the automated classification of protein sequences with modular architecture. *BMC Bioinfo* **6:** 216.

Stamatakis A. 2014. RAxML version 8: a tool for phylogenetic analysis and post-analysis of large phylogenies. *Bioinfo* **30:** 1312-1313.

Stanke M, Keller O, Gundunz I, Hayes A, Waack S, Morgenstern B. 2006. AUGUSTUS: *ab initio* prediction of alternative transcripts. *Nucl Ac Res* **34:** W435-439.

Strauss HM, Keller S. 2008. Pharmacological interference with protein-protein interactions mediated by coiled-coil motifs. *Hand Exp Pharmacol* **186:** 461-482.

Stringer JR. 2007. Antigenic Variation in *Pneumocystis*. *J Eukaryot Microbiol* **54:** 8-13.

Sunkin SM, Stringer JR. 1996. Translocation of surface antigen genes to a unique telomeric expression site in *Pneumocystis carinii*. *Mol Microbiol* **19:** 283-295 .

Thomas CF JR., Loef EB, Limper AH. 1999. Analysis of *Pneumocystis carinii* introns. *Infect Immun* **67:** 6157-6160.

Turan S, Bode J. 2011. Site-specific recombinases: from tag-and-target- to tag-and-exchange-based genomic modifications. *FASEB J* **25:**4088-4107.

Wada M, Nakamura Y. 1996. Unique telomeric expression site of major-surface-glycoprotein genes of *Pneumocystis carinii*. *DNA Res* **3:** 55-64.

Waterhouse AM, Procter JB, Martin DM, Clamp M, Barton GJ. 2009. Jalview version 2-a multiple sequence alignment and analysis workbench. *Bioinfo* **25:**1189-1191.

Williamson MP. 1994. The structure and function of proline-rich regions in proteins. *Biochem J* **297:** 249-260.

506 Yu G, Smith DK, Zhu H, Guan Y, Lam TT-Y. 2017. GGTREE: an R package for visualization
507 and annotation of phylogenetic trees with their covariates and other associated data. *Meth*
508 *Ecol Evol 8:* 28-36.